

ATLAS Roman Pots

General Experimental Overview

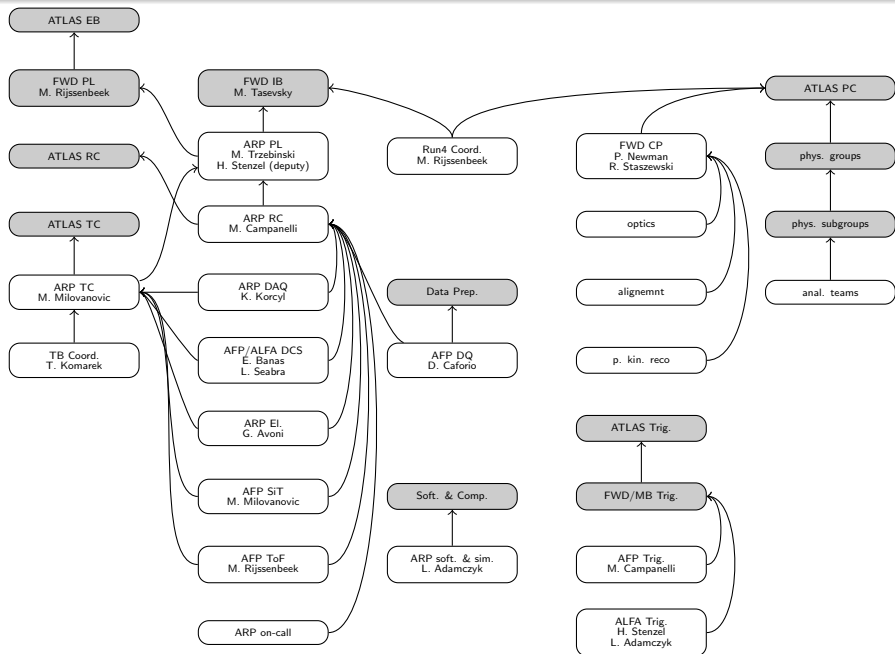
Maciej Trzebiński

Institute of Nuclear Physics
Polish Academy of Sciences

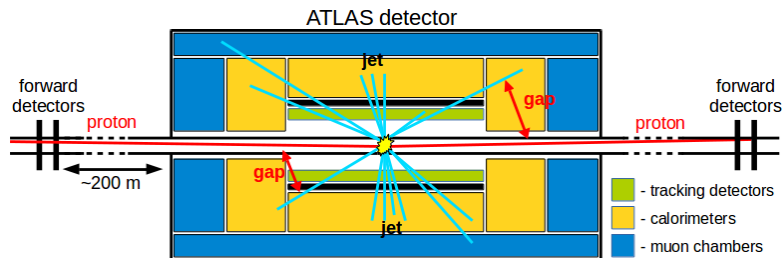


Photon-induced processes
IPPP Durham, 3rd November 2022

View of ATLAS Roman Pots Organization



Assumption: one would like to measure diffractive interactions at the LHC.
Typical diffractive topology: a gap in rapidity is present between proton(s) and central system and one or both interacting proton stay intact.

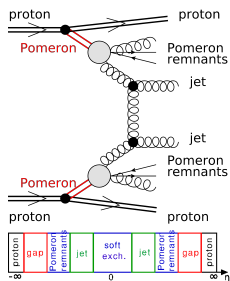


Method 1 (rapidity gap):

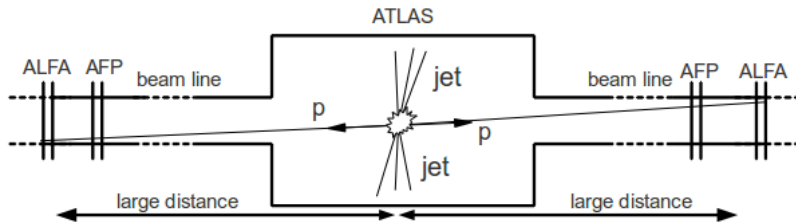
- + usual method of diffractive pattern recognition
- + no need to install additional detectors
- gap may be killed by e.g. particles from pile-up
- gap may be outside acceptance of central detector

Method 2 (forward protons):

- + protons are directly measured
- + can be used in pile-up environment
- protons are scattered at small angles (few μrad)
- additional "forward" detectors are needed far away from the interaction point



Intact protons → natural diffractive signature → usually scattered at very small angles (μrad) → detectors must be located far from the Interaction Point.

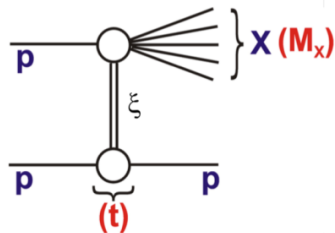


ALFA

- **A**bsolute **L**uminosity **F**or **A**TLAS
- 240 m from ATLAS IP
- soft diffraction (elastic scattering)
- special runs (high β^* optics)
- vertically inserted Roman Pots
- tracking detectors, resolution:
 $\sigma_x = \sigma_y = 30 \mu\text{m}$

AFP

- **A**TLAS **F**orward **P**roton
- 210 m from ATLAS IP
- hard diffraction
- nominal runs (collision optics)
- horizontally inserted Roman Pots
- tracking detectors, resolution:
 $\sigma_x = 6 \mu\text{m}, \sigma_y = 30 \mu\text{m}$
- timing detectors, resolution:
 $\sigma_t \sim 25 \text{ps}$



- t – squared four-momentum transferred from the proton:

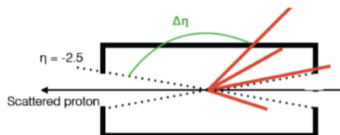
$$t \approx -p_T^2$$

- p_T – proton transverse momentum
- ξ – momentum fraction of the proton carried by the Pomeron:

$$\xi = 1 - E/E_{beam}$$

$$\xi \approx \sum_i (E^i \pm p_z^i) / \sqrt{s}$$

- $\Delta\eta$ – pseudorapidity gap – space in which no particles are produced / detected

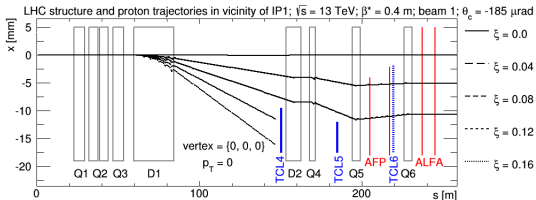


Optics

Proton trajectory is determined by the LHC magnetic field.

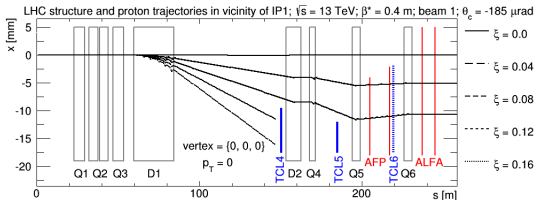
Proton trajectory is determined by the LHC magnetic field.

collision optics,
ALFA and **AFP**:
 trajectory due to ξ
 $\xi = 1 - E_{proton}/E_{beam}$

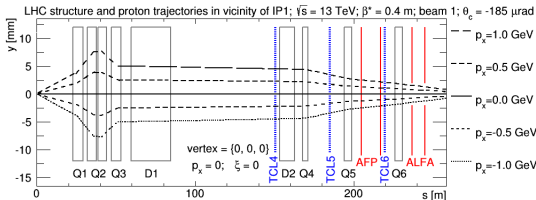


Proton trajectory is determined by the LHC magnetic field.

collision optics,
ALFA and AFP:
trajectory due to ξ
 $\xi = 1 - E_{proton}/E_{beam}$

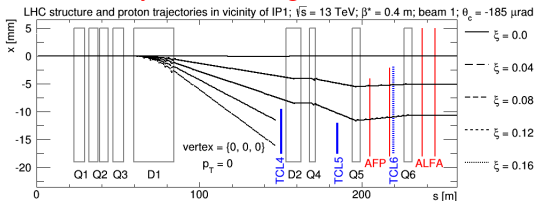


collision optics,
ALFA and AFP:
trajectory due to p_y

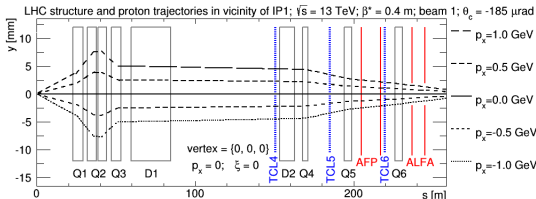


Proton trajectory is determined by the LHC magnetic field.

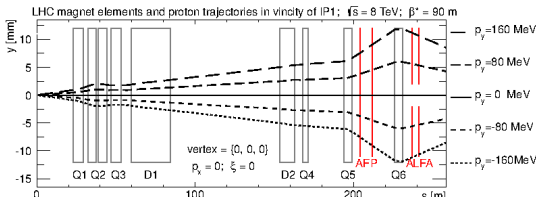
collision optics,
ALFA and AFP:
trajectory due to ξ
 $\xi = 1 - E_{proton}/E_{beam}$



collision optics,
ALFA and AFP:
trajectory due to p_y



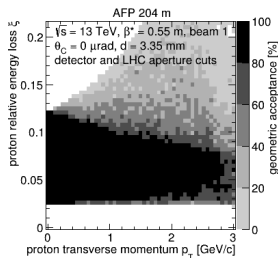
special high- β^* optics,
ALFA:
improve acceptance in
 $p_T = \sqrt{p_x^2 + p_y^2}$



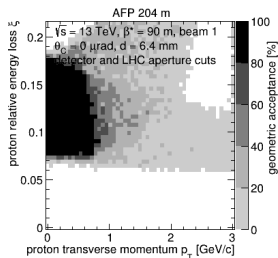
From SPIE 9290 (2014) 929026, arXiv:1408.1836

Geometric Acceptance for Various Optics

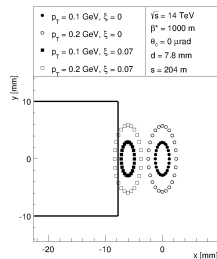
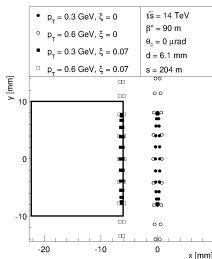
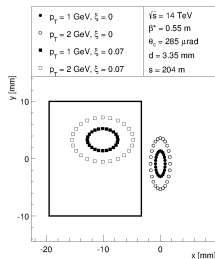
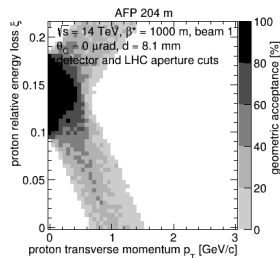
$\beta^* = 0.55$ m
nominal (*collision*)



$\beta^* = 90$ m
special (*high- β^**)



$\beta^* = 1000$ m
special (*high- β^**)

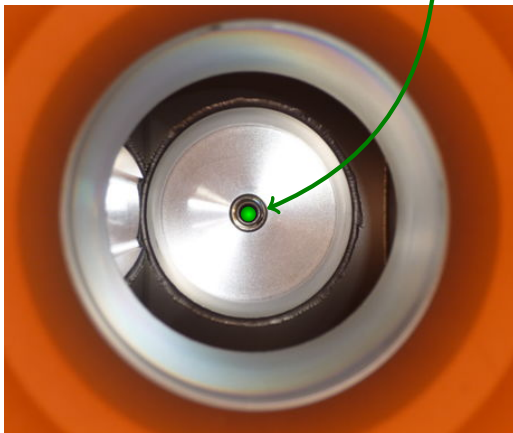


Simulation: distance from the beam was set to 10σ ($\beta^* = 0.55$ m) or 15σ ($\beta^* = 90$ and 1000 m).

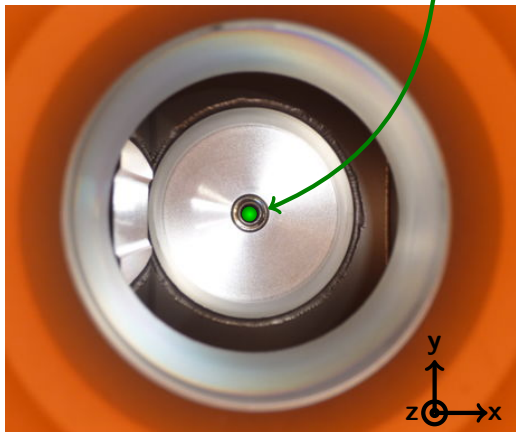
From SPIE 9290 (2014) 929026, arXiv:1408.1836



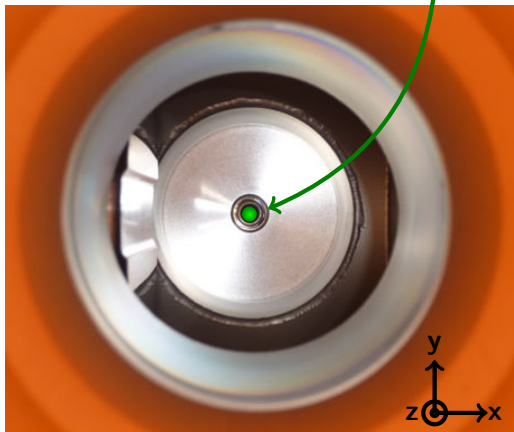
LHC beam



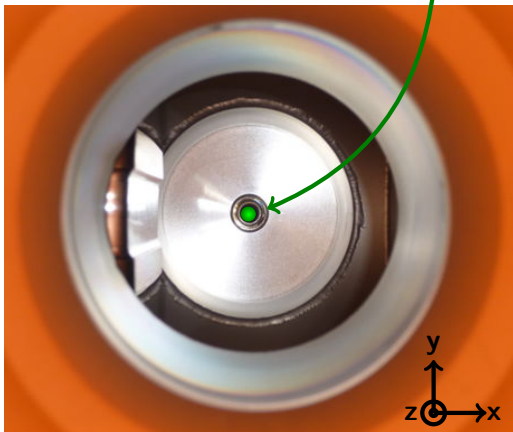
LHC beam



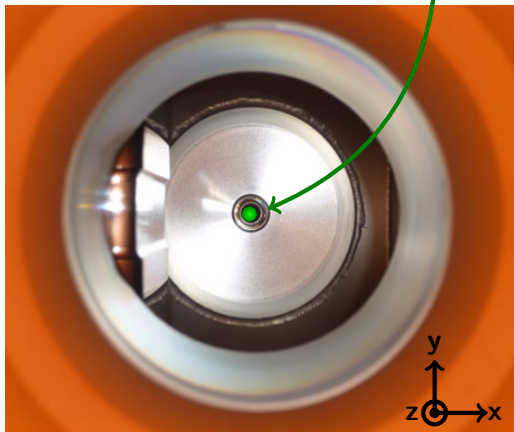
LHC beam



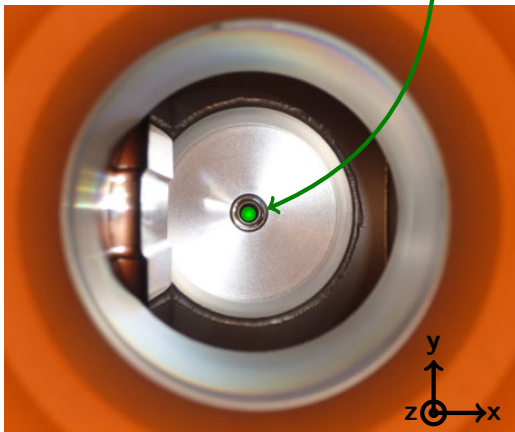
LHC beam



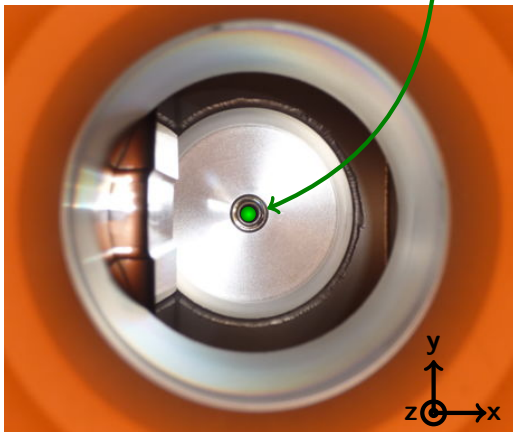
LHC beam



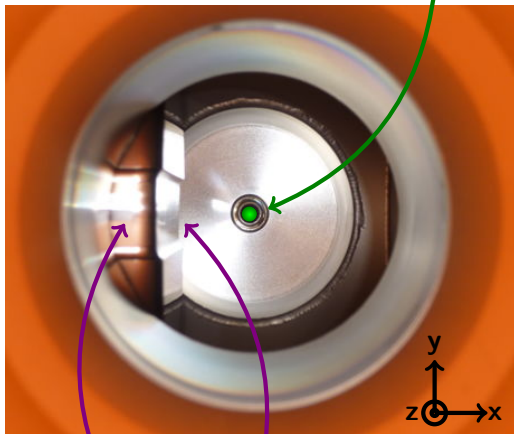
LHC beam



LHC beam



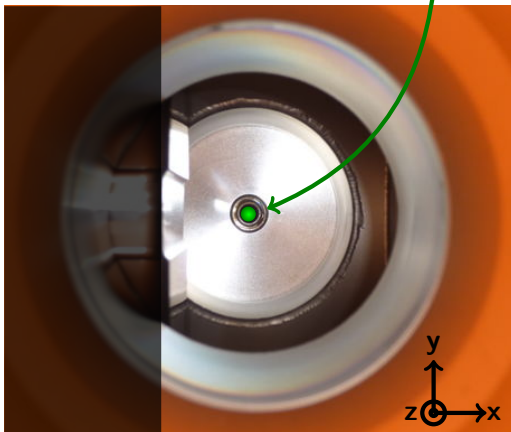
LHC beam



thin window and floor (300 μm)

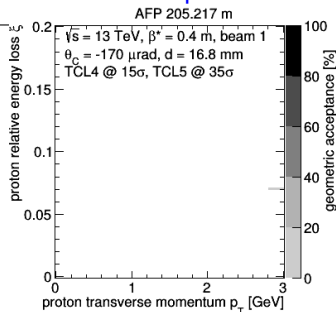
shadow of TCL4 and TCL5 collimators

LHC beam

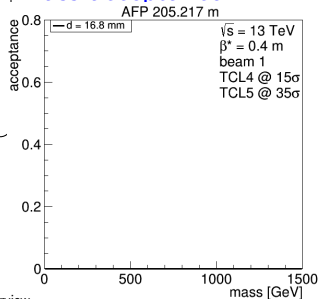


thin window and floor ($300 \mu\text{m}$)

Geometric acceptance:

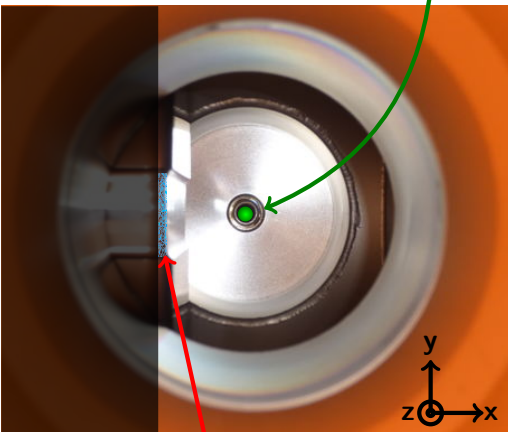


Mass acceptance:



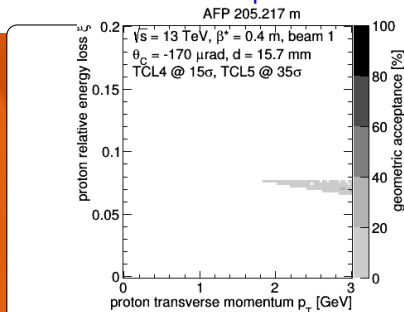
shadow of TCL4 and TCL5 collimators

LHC beam

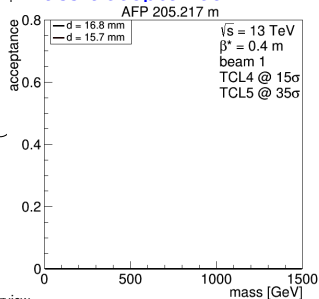


diffractive protons
thin window and floor ($300 \mu\text{m}$)

Geometric acceptance:

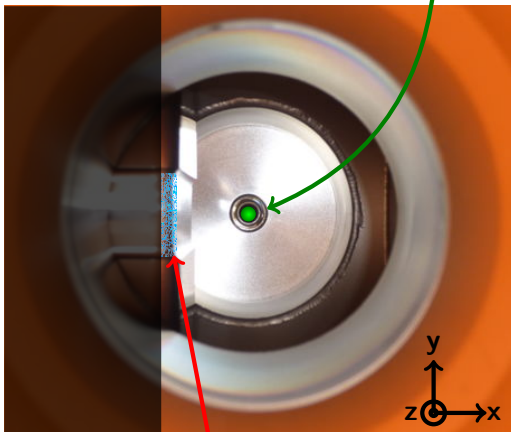


Mass acceptance:



shadow of TCL4 and TCL5 collimators

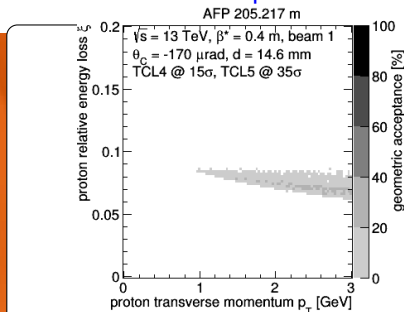
LHC beam



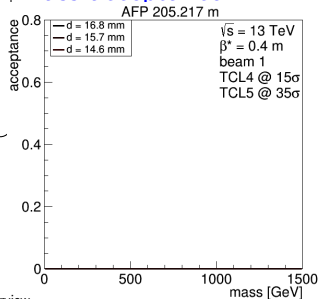
diffractive protons

thin window and floor ($300 \mu\text{m}$)

Geometric acceptance:

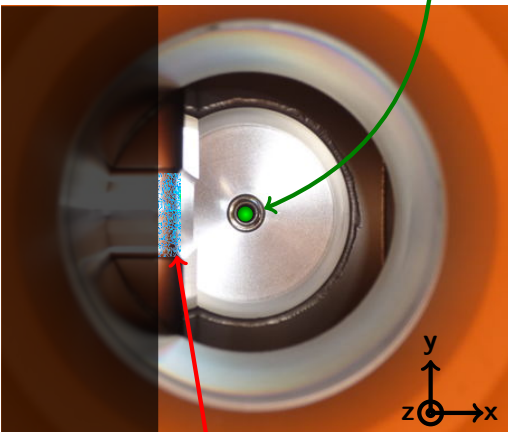


Mass acceptance:



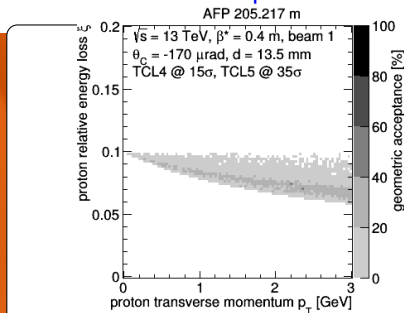
shadow of TCL4 and TCL5 collimators

LHC beam

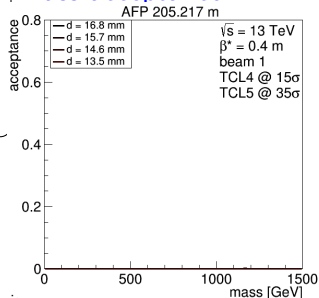


diffractive protons
thin window and floor ($300 \mu\text{m}$)

Geometric acceptance:

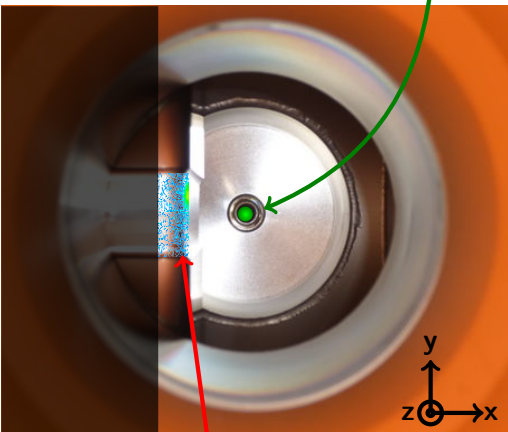


Mass acceptance:



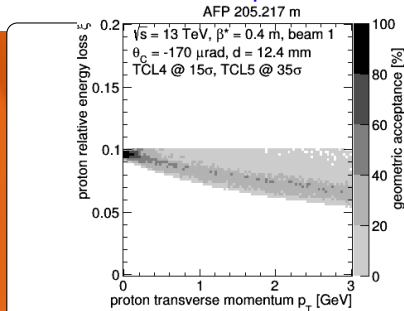
shadow of TCL4 and TCL5 collimators

LHC beam

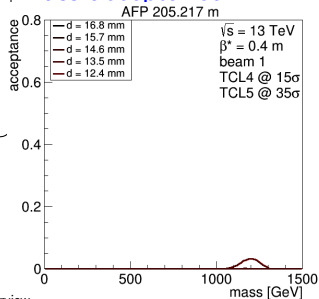


diffractive protons
thin window and floor ($300 \mu\text{m}$)

Geometric acceptance:

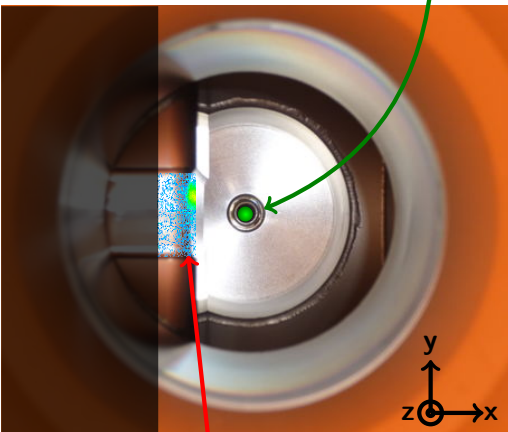


Mass acceptance:



shadow of TCL4 and TCL5 collimators

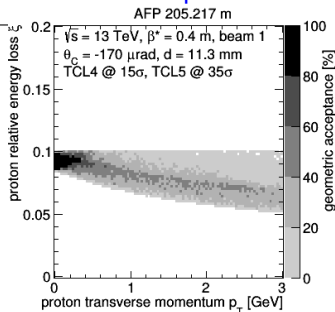
LHC beam



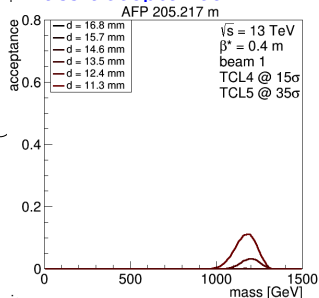
diffractive protons

thin window and floor ($300 \mu\text{m}$)

Geometric acceptance:

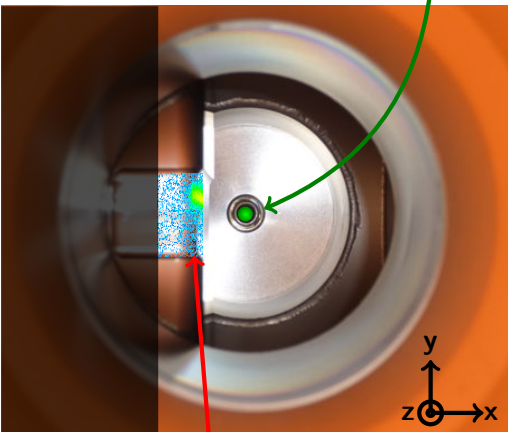


Mass acceptance:



shadow of TCL4 and TCL5 collimators

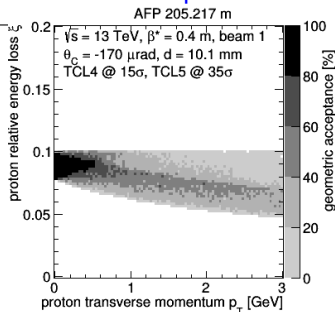
LHC beam



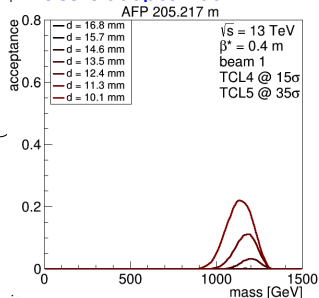
diffractive protons

thin window and floor ($300 \mu\text{m}$)

Geometric acceptance:

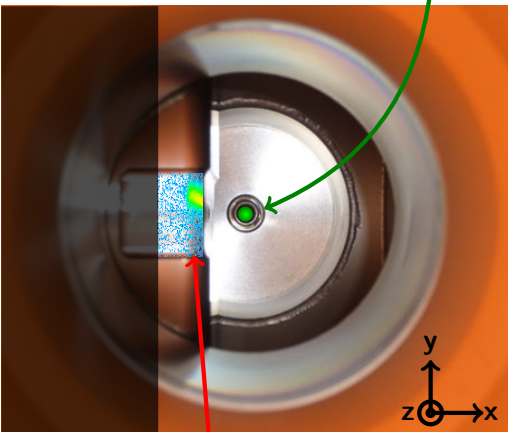


Mass acceptance:



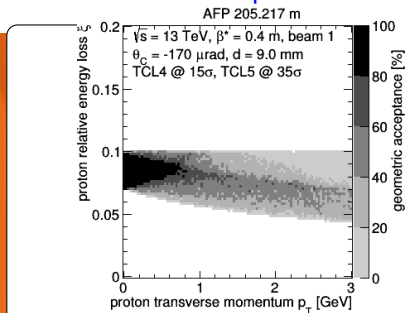
shadow of TCL4 and TCL5 collimators

LHC beam

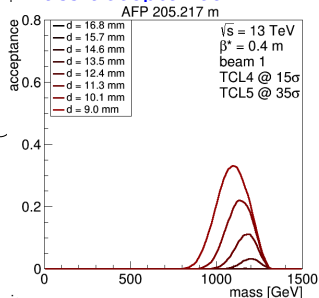


diffractive protons
thin window and floor ($300 \mu\text{m}$)

Geometric acceptance:

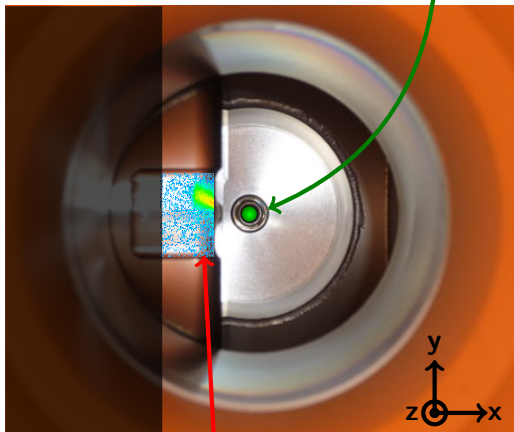


Mass acceptance:



shadow of TCL4 and TCL5 collimators

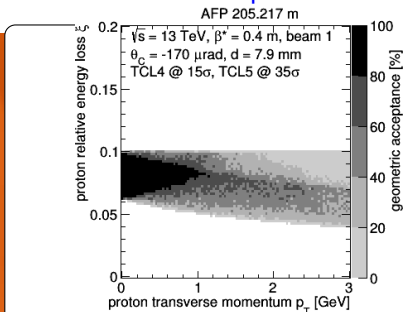
LHC beam



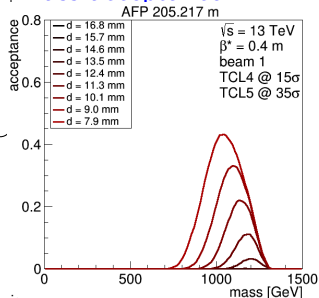
diffractive protons

thin window and floor ($300 \mu\text{m}$)

Geometric acceptance:



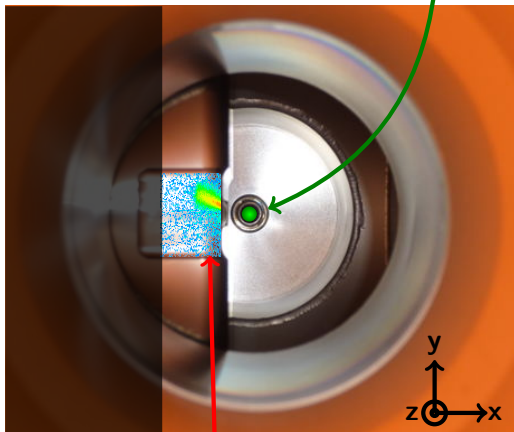
Mass acceptance:



shadow of TCL4 and TCL5 collimators

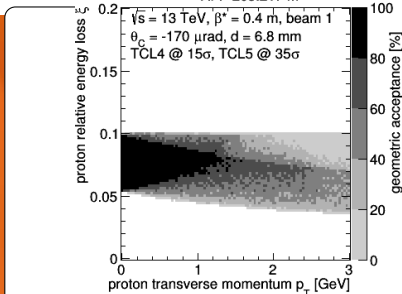
LHC beam

Geometric acceptance:

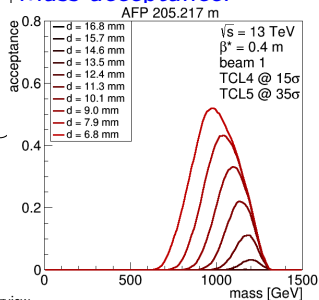


diffractive protons

thin window and floor ($300 \mu\text{m}$)

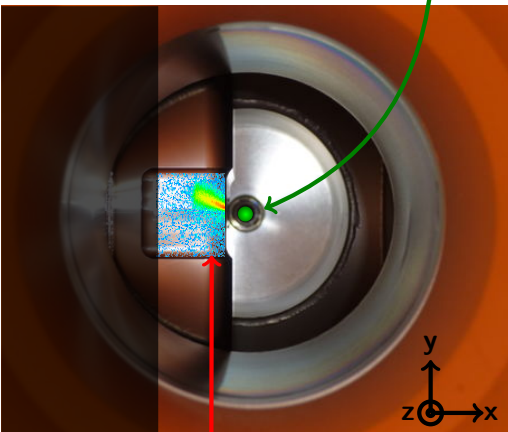


Mass acceptance:



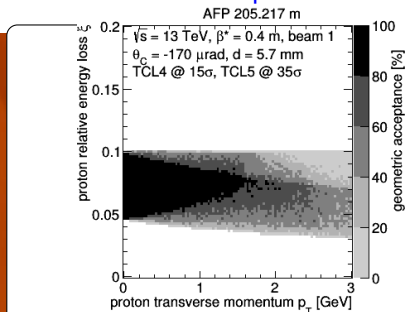
shadow of TCL4 and TCL5 collimators

LHC beam

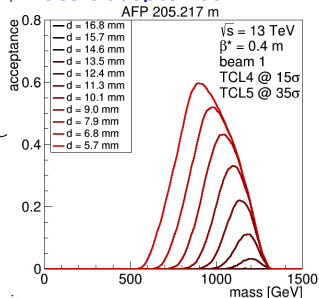


diffractive protons
thin window and floor ($300 \mu\text{m}$)

Geometric acceptance:

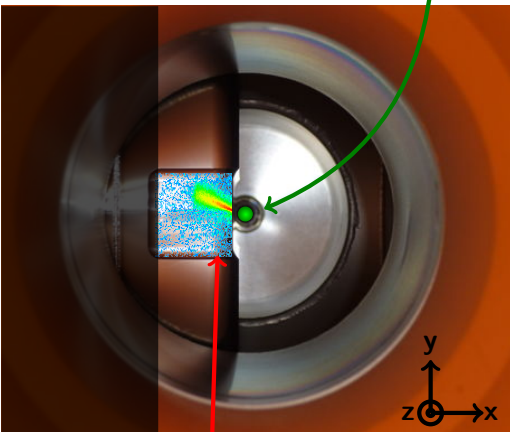


Mass acceptance:



shadow of TCL4 and TCL5 collimators

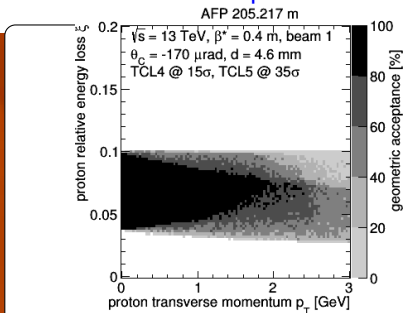
LHC beam



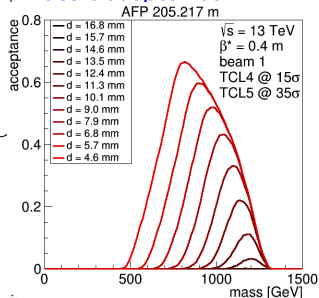
diffractive protons

thin window and floor ($300 \mu\text{m}$)

Geometric acceptance:

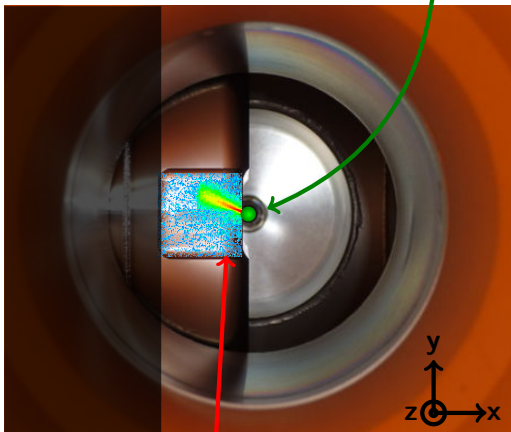


Mass acceptance:



shadow of TCL4 and TCL5 collimators

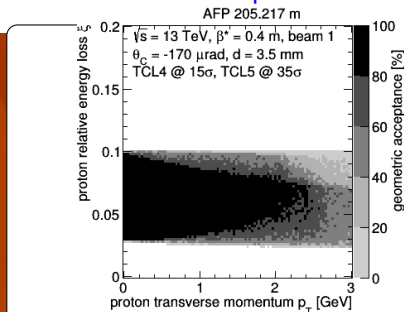
LHC beam



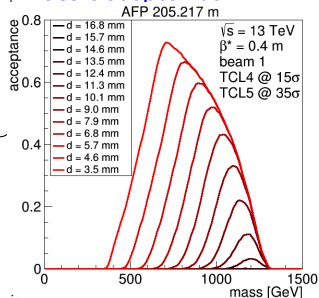
diffractive protons

thin window and floor ($300 \mu\text{m}$)

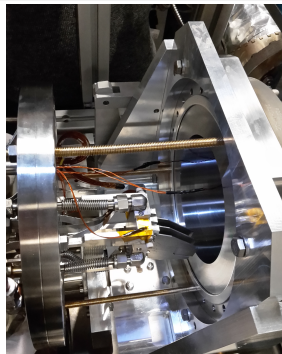
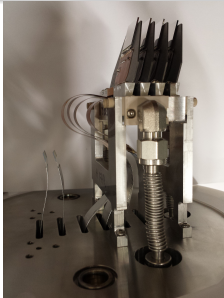
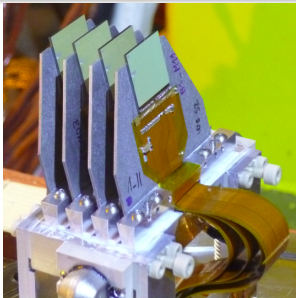
Geometric acceptance:



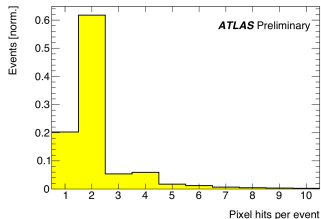
Mass acceptance:



Detectors

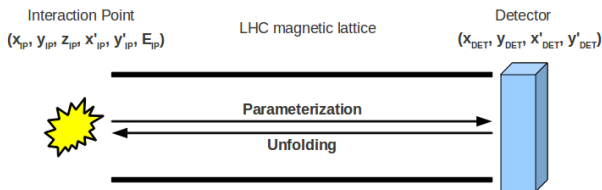


- Four detectors in each station.
- Technology: slim-edge 3D ATLAS IBL pixel sensors bonded with FE-I4 readout chips.
- Pixel size: $50 \times 250 \mu\text{m}^2$.
- Tilted by 14° to improve resolution in x .
- Resolution: $\sim 6 \mu\text{m}$ in x and $\sim 30 \mu\text{m}$ in y .
- Trigger: majority vote (2 out of 3; two chips in FAR station are paired and vote as one).
- No major changes between Run 2 and Run 3 detector setups.

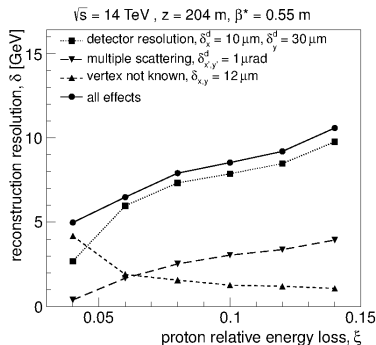


From JINST 11 (2016) P09005;
JINST 12 (2017) C01086

Proton Tagging or Position Measurement?

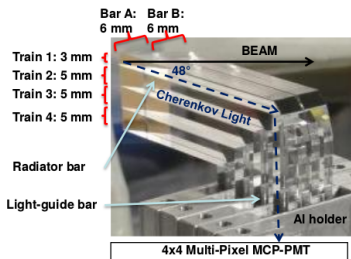


- At the interaction point proton (IP) is fully described by six variables: position (x_{IP}, y_{IP}, z_{IP}) , angles (x'_{IP}, y'_{IP}) and energy (E_{IP}) .
- They translate to unique position at the forward detector $(x_{DET}, y_{DET}, x'_{DET}, y'_{DET})$.
- **Idea:** get information about proton kinematics at the IP from their position in the AFP detector.
- **Exclusivity:** kinematics of scattered protons is strictly connected to kinematics of central system.
- **Detector resolution** play important role in precision of such method.

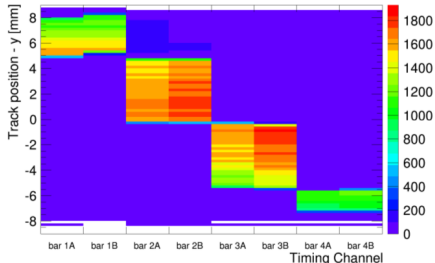


From ISRN High Energy Physics (2012)
491460; ATLAS-TDR-024

ToF LQbars

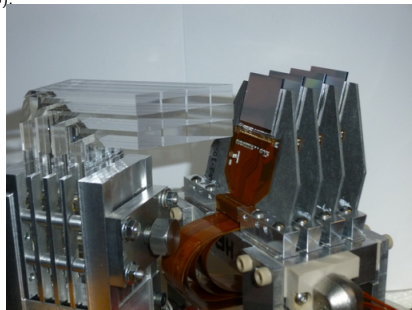


Tracking-Timing correlation y

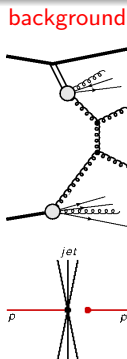
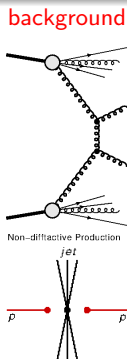
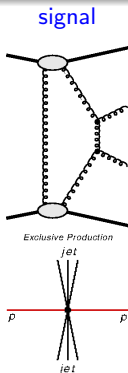


Setup and performance shown above are from test-beam (Opt. Express **24** (2016) 27951, JINST **11** (2016) P09005).

- 4x4 quartz bars oriented at the Cherenkov angle with respect to the beam trajectory.
- Light is directed to Photonis MCP-PMT.
- Expected resolution: ~ 25 ps.
- Installed in both FAR stations.

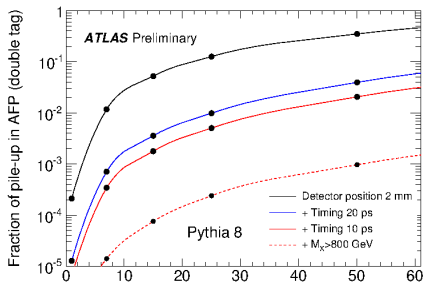


Pile-up Background Reduction

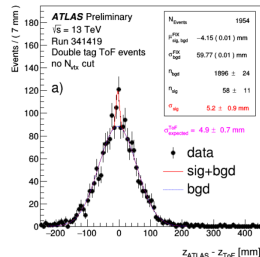
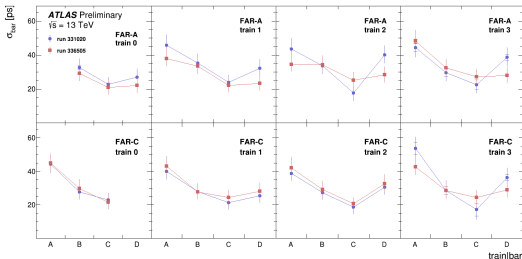
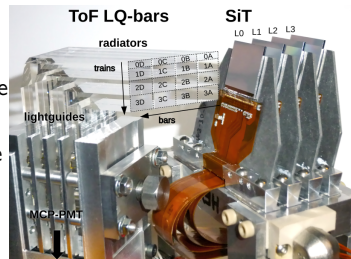


Idea:

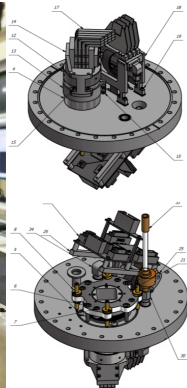
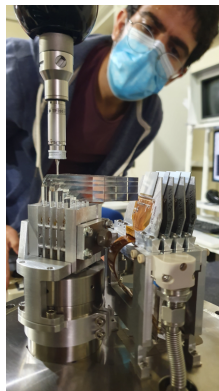
- measure difference of time of flight of scattered protons, $(t_A - t_C)/2$
- compare to vertex reconstructed by central detector, $(t_A - t_C) \cdot c/2 - z_{\text{central}}$



- Performance analysis based on 2017 data (taken with $\mu \approx 2$): [ATL-FWD-PUB-2021-002](#).
- Poor efficiency of few percent due to fast PMT degradation; effect not expected during Run 3 due to new PMTs.
- Very good timing resolution: 20 – 50 ps for single bar.
- Overall time resolution of each ToF detector:
 - 20 ± 4 ps for side A,
 - 26 ± 5 ps for side C,
 - note: systematic uncertainties dominate.



- Improvement in silicon detector cooling (new heat exchangers).
- Production of new tracking modules.
- New design of detector flange: **Out-of-Vacuum solution for ToF detectors**
- New trigger module: possibility to trigger on single train.
- New photo-multipliers: address inefficiency issues from Run2 data-taking.
- Above items were successfully tested at DESY in 2020.



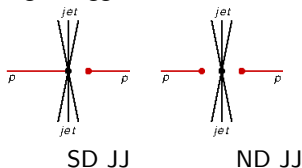
Both NEAR and FAR station have been successfully installed:

- laser survey (positioning wrt. LHC) done,
- interlock validation done → Roman pots qualified to be inserted to take data,
- SiT readout and trigger commissioned,
- ToF commissioning ongoing,
- successful data-taking during high- and low- μ runs in 2022.

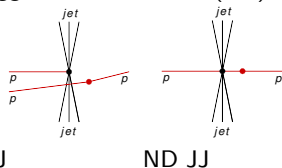
Backgrounds

Probability of Single and Double Tag

Single Tagged Soft Interaction(ST)

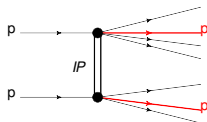
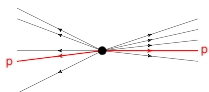


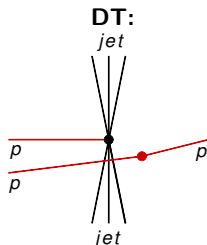
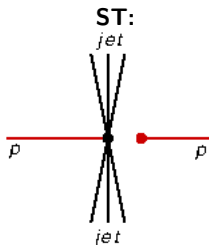
Double Tagged Soft Interaction(DT)



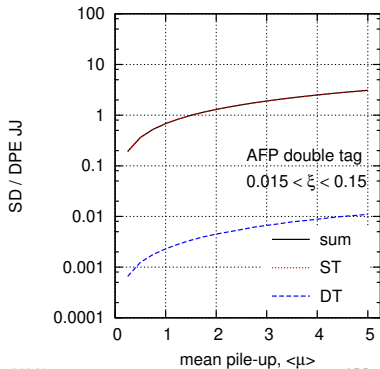
Process (PYTHIA8)	Single Tag		Double Tag	
	probability	cross-section [mb]	probability	cross-section [μb]
SD	0.18	2.32	$4.5 \cdot 10^{-4}$	5.8
DD	0.051	0.45	$4.3 \cdot 10^{-4}$	3.8
ND	0.0054	0.31	$1.4 \cdot 10^{-5}$	0.8
MB	0.039	3.10	$1.4 \cdot 10^{-4}$	10.4

Note: Double Diffractive Dissociation with protons from hadronisation propagating in forward direction.

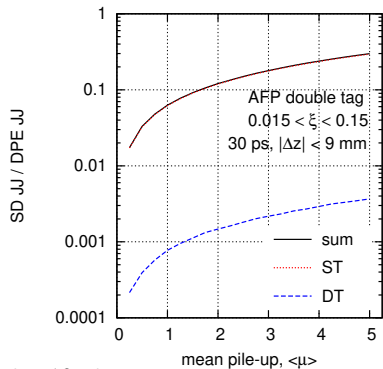




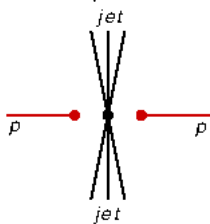
Single Diffractive contribution



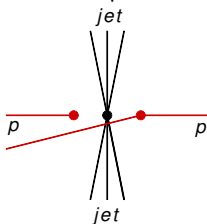
Single Diffractive contribution timing cut



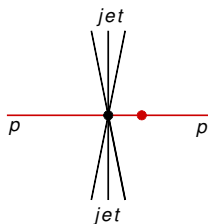
ST + ST:



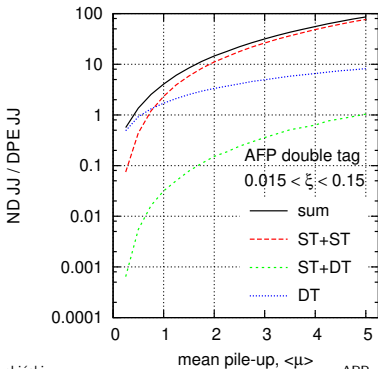
ST + DT:



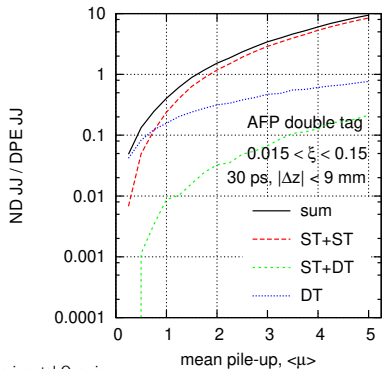
DT:

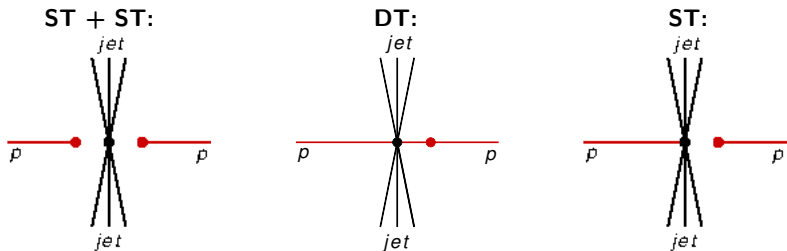


Non-Diffractive contribution

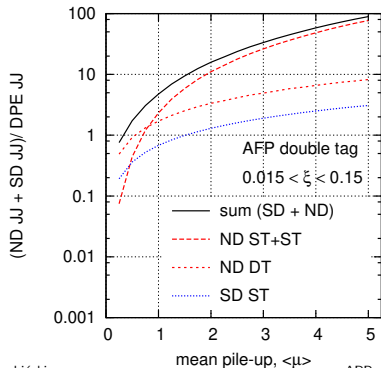


Non-Diffractive contribution timing cut

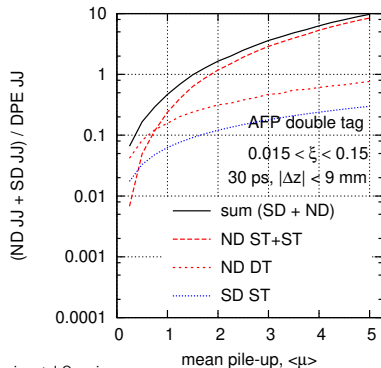




ND + SD contribution

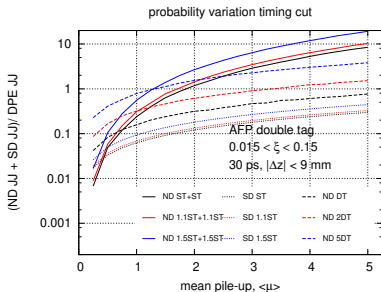
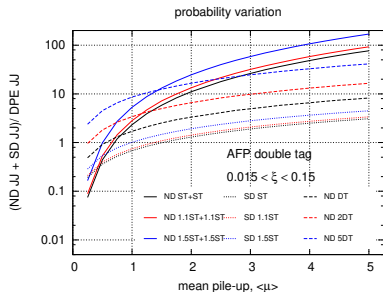


SD+ND contribution timing cut



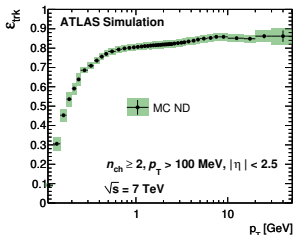
What happens if the Single and Double Tag Probabilities are higher than predicted by MC generators?

Probability	
Single Tag	Double Tag
0.039	$1.4 \cdot 10^{-4}$
1.1 · 0.039	2 · $1.4 \cdot 10^{-4}$
1.5 · 0.039	5 · $1.4 \cdot 10^{-4}$

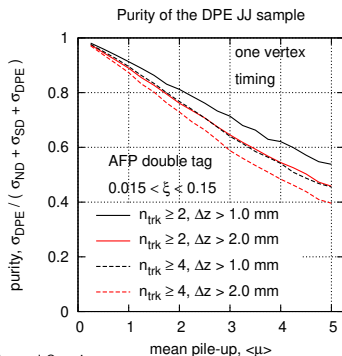
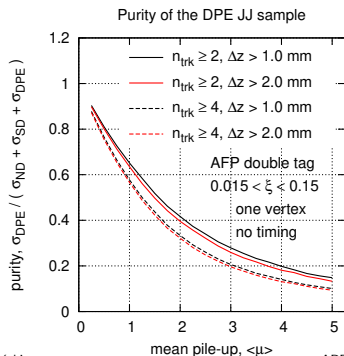


Two inefficiency sources:

- soft vertex is merged with a hard one ($\Delta z = 1$ mm, $\Delta z = 2$ mm),
- not enough reconstructed tracks pointing to the soft vertex ($n_{trk} = 2$, $n_{trk} = 4$).



Min. number of tracks	SD	DD	Probability ND	min-bias
2	0.532	0.601	0.995	0.876
3	0.494	0.540	0.985	0.855
4	0.457	0.483	0.968	0.831
5	0.419	0.429	0.944	0.801



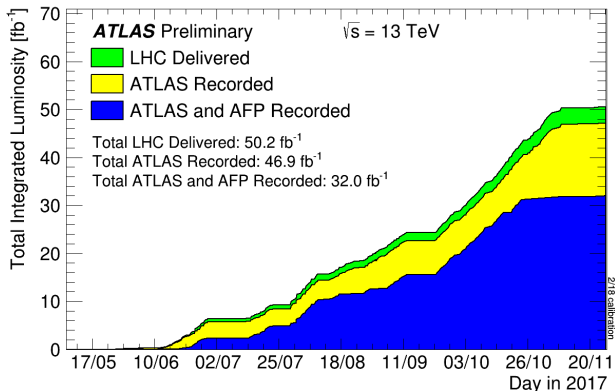
Data Samples

2016

- Conditions: $\sqrt{s} = 13$ TeV, $\beta^* = 0.4$ m
- Only two stations installed (ATLAS side C).
- Only single tagged events.
- Data taken during BBA:
 - two runs,
 - closer to the beam than during standard collisions,
 - very useful for alignment and optics studies.
- Data taken during special runs:
 - $\mu \sim 0.03$:
 - int. lumi.: ~ 40 nb $^{-1}$,
 - AFP triggers: ~ 2 kHz stored,
 - main goal: soft diffraction.
 - $\mu \sim 0.3$:
 - int. lumi.: ~ 500 nb $^{-1}$,
 - AFP triggers: ~ 2 kHz stored,
 - main goal: low- p_T jets.
- Data taken during standard runs:
 - AFP was inserted only when number of bunches was not greater than 600 (ramp-up).

2017


- $\sqrt{s} = 13$ TeV, $\beta^* = 0.3$ and 0.4 m
- Full system ready.
- Single and double tagged events.
- Data taken during BBA:
 - two runs.
- Data taken during special runs:
 - $\mu \sim 0.05$:
 - int. lumi.: ~ 65 nb $^{-1}$,
 - AFP triggers: ~ 2 kHz stored,
 - main goal: soft diffraction.
 - $\mu \sim 1$:
 - int. lumi.: ~ 640 nb $^{-1}$,
 - AFP triggers: ~ 2 kHz stored,
 - main goal: low- p_T jets.
 - $\mu \sim 2$:
 - int. lumi.: ~ 150 pb $^{-1}$,
 - AFP triggers: ~ 300 Hz stored,
 - goals: medium- p_T jets, W/Z .
- Data taken during standard runs:
 - AFP was inserted on regular basis, usually few minutes after stable beams.



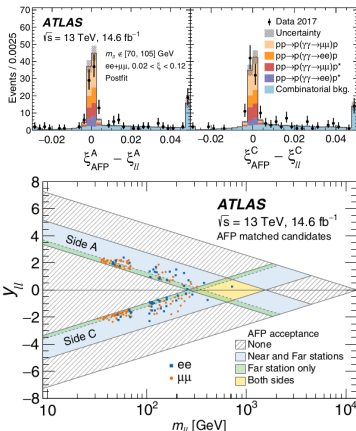
- This is only ATLAS and AFP recorded – there are no corrections due to efficiency of subsystems, etc.
- ToF trigger and detector were suffered very low efficiency → analysis should base on proton tagging rather than on ToF background reduction.

Observation and Measurement of Forward Proton Scattering in Association with Lepton Pairs Produced via the Photon Fusion Mechanism at ATLAS

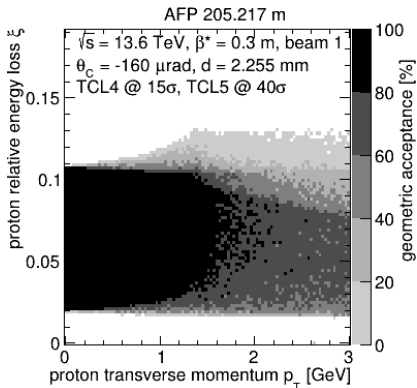
G. Aad *et al.*^{*}
(ATLAS Collaboration)

 (Received 2 October 2020; revised 30 October 2020; accepted 23 November 2020; published 23 December 2020)

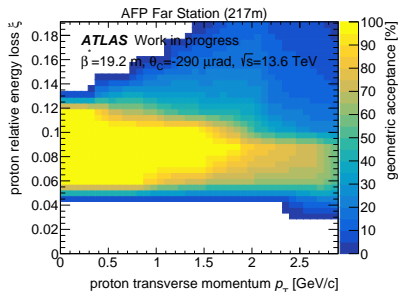
- Exclusive di-muons, $pp \rightarrow p l^- l^+ p$:
 - proton(s) measured in AFP,
 - leptons ($\mu^+ \mu^-$ or $e^+ e^-$) measured in ATLAS.
- 2017 data; $\sqrt{s} = 13$; $L = 14.6 \text{ fb}^{-1}$.
- Powerful background rejection due to AFP:
 - proton tagging,
 - kinematics match: proton vs lepton system.
- 57 (123) candidates in the $ee + p$ ($\mu\mu + p$) final state.
- Background-only hypothesis rejected with a significance exceeding 5σ in each channel.
- Measured cross sections:
 - $\sigma_{ee+p} = 11.0 \pm 2.6(\text{stat}) \pm 1.2(\text{syst}) \pm 0.3(\text{lumi})$,
 - $\sigma_{\mu\mu+p} = 7.2 \pm 1.6(\text{stat}) \pm 0.9(\text{syst}) \pm 0.2(\text{lumi})$.

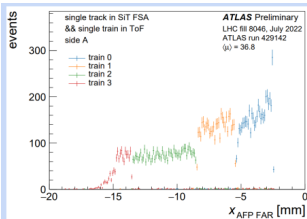


Low- β^* Runs

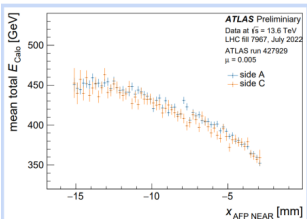
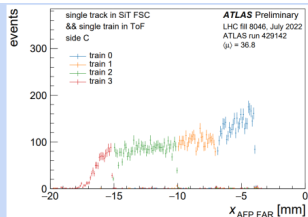


LHCf Runs

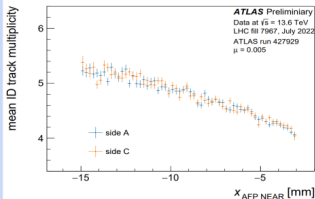




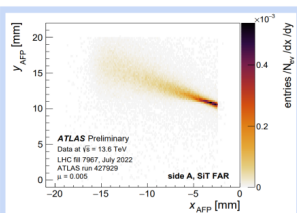
The x position of the track reconstructed in AFP SiT (FAR station) in events in which a single-train signal in ToF detector was observed for side A (left plot) and side C (right plot). The differences in the $x_{\text{AFP FAR}}$ between sides are due to global alignment corrections not being applied).



Correlation between the x position of reconstructed tracks in AFP NEAR stations and the total energy measured by the ATLAS Calorimeters for side A and C.

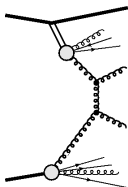


Correlation between the x position of reconstructed tracks in AFP NEAR stations and the charged track multiplicity in the ATLAS Inner Detector for Side A and C.



Positions of tracks reconstructed in AFP. Coordinate system: center of the beampipe at $(x, y) = (0, 10 \text{ mm})$

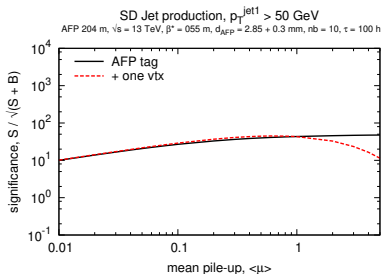
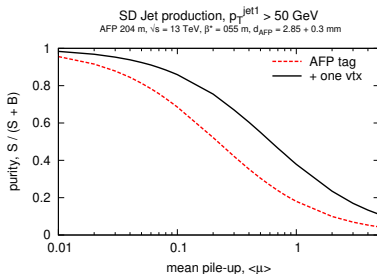
Hard Diffractive Processes



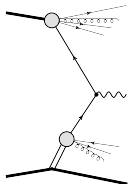
Motivation:

- measure cross section and gap survival probability,
- search for the presence of an additional contribution from Reggeon exchange,
- check Pomeron universality between ep and pp colliders.

Example: purity and statistical significance for AFP and $\beta^* = 0.55$ m.



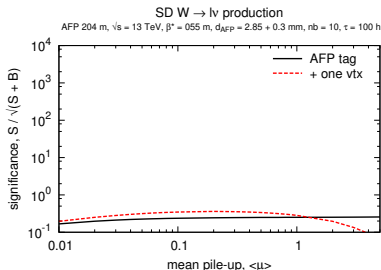
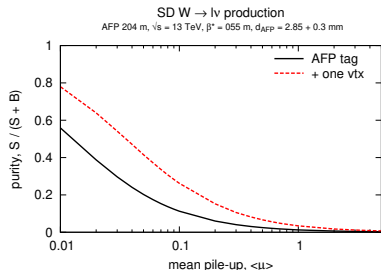
More details in: J. Phys. G: Nucl. Part. Phys. **43** (2016) 110201



Motivation:

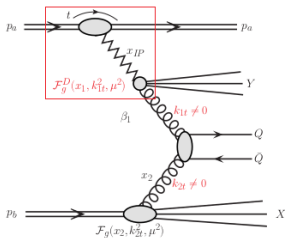
- measure cross section and gap survival probability,
- measure Pomeron structure and flavor composition,
- search for charge-asymmetry.

Example: $W \rightarrow l\nu$ – purity and stat. significance for AFP and $\beta^* = 0.55$ m.



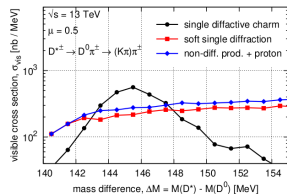
W asymmetry studies published in: Phys.Rev. D **84** (2011) 114006

More details in: J. Phys. G: Nucl. Part. Phys. **43** (2016) 110201

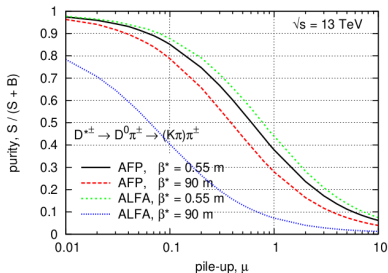
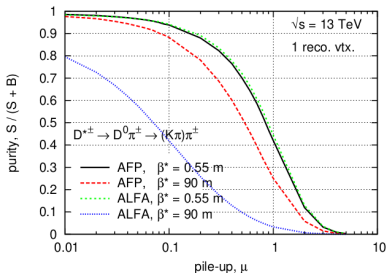


Motivation:

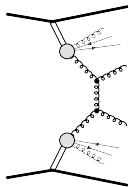
- measure cross section and gap survival probability,
- test the k_t -factorization approach.



Example: purity ALFA and AFP for $\beta^* = 0.55$ and 90 m with and without 1 vertex requirement.

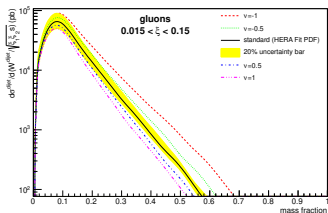


More details in: J. High Energ. Phys. **2017** (2017) 89

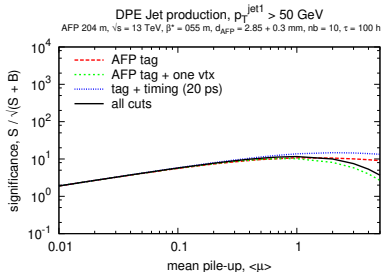
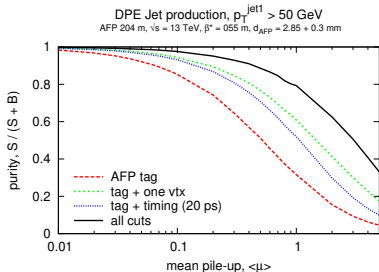


Motivation:

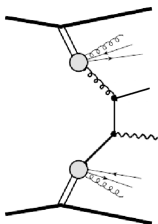
- measure cross section and gap survival probability,
- search for the presence of an additional contribution from Reggeon exchange,
- investigate gluon structure of the Pomeron.



Example: purity and statistical significance for AFP and $\beta^* = 0.55$ m.

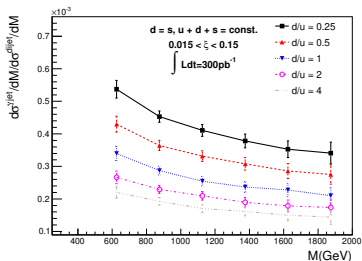
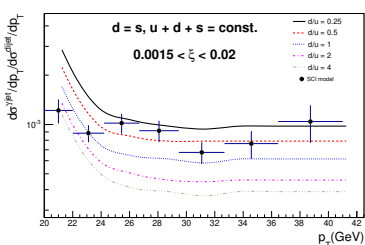


More details in: J. Phys. G: Nucl. Part. Phys. **43** (2016) 110201



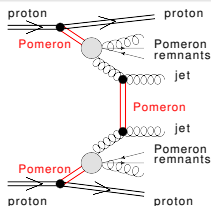
Motivation:

- measure cross section and gap survival probability,
- sensitive to quark content in Pomeron (at HERA it was assumed that $u = d = s = \bar{u} = \bar{d} = \bar{s}$).



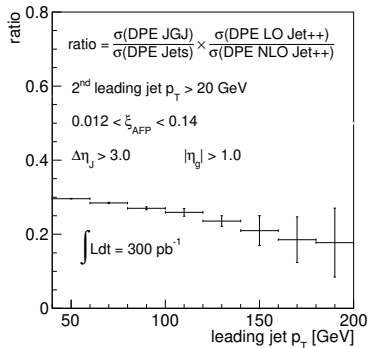
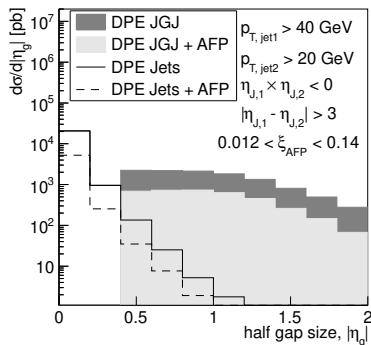
More details in: Phys.Rev. D **88** (2013) 7, 074029

Double Pomeron Exchange Jet-Gap-Jet Production

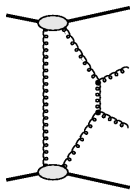


Motivation:

- measure cross section and gap survival probability,
- test BFKL model.



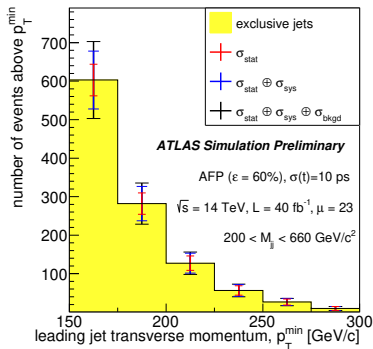
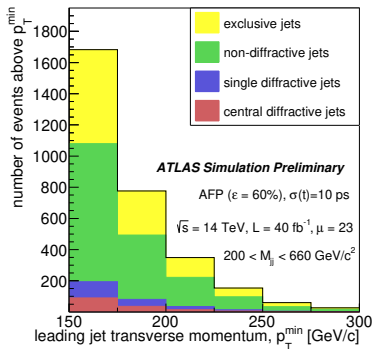
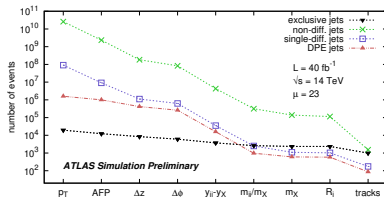
More details in: Phys.Rev. D **87** (2013) 3, 034010



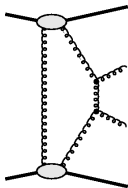
Exclusive Production

Motivation:

- cross section measurement,
- constrain other exclusive productions (e.g. Higgs).



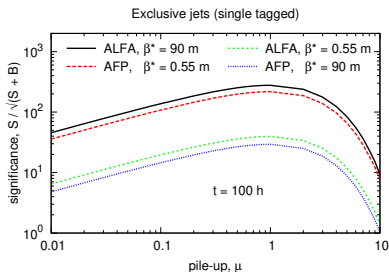
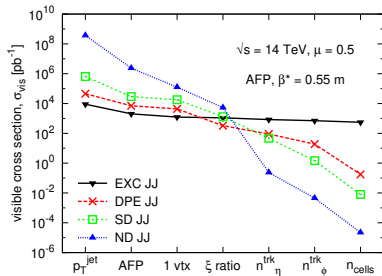
Public ATLAS note: ATL-PHYS-PUB-2015-003



Exclusive Production

Motivation:

- cross section measurement,
- constrain other exclusive productions (e.g. Higgs).



More details in: Eur. Phys. J. C **75** (2015) 320
and Acta Phys. Pol. B **47** (2016) 1745

● According to HL-LHC machine layout only few locations are possible:

- RP1A at 195.5 m
- RP2A at 217.0 m
- RP3A at 234.0 m
- RP1B at 198.0 m
- RP2B at 219.5 m
- RP3B at 237.0 m
- RP3C at 245.0 m

● Collimators are also relocated:

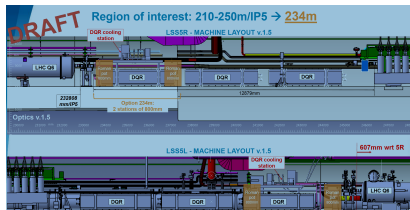
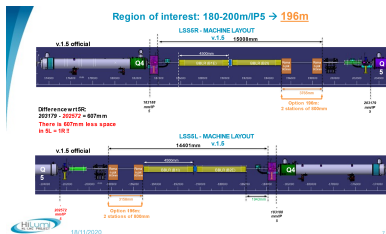
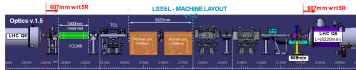
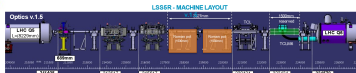
- TCLPX4 at 136 m
- TCL5 at 199 m
- TCL6 at 221 m

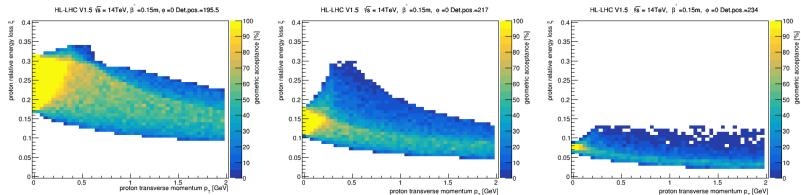
● Studies were done using newest available HL-LHC optics.

● Assumption:

- $\sqrt{s} = 14 \text{ TeV}$, $\beta^* = 15 \text{ cm}$,
- crossing angle of $250 \mu\text{rad}$ with phase: $\phi = 0$,
- emittance $\epsilon = 2.5 \mu\text{m} \cdot \text{rad}$.

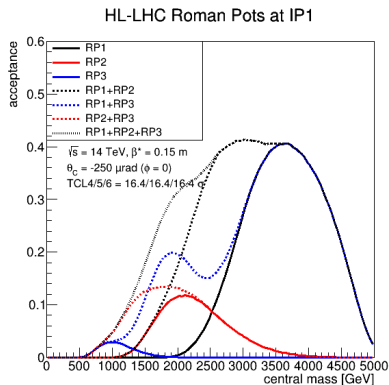
Region of interest: 210-250m/IP5 → 220m





- Proton relative energy loss: $\xi = 1 - \frac{E_{proton}}{E_{beam}}$.
- High- ξ limit on acceptance is due to beampipe elements and TCL collimators between collision point and Roman pot.
- Low- ξ limit is due to detector-beam distance, which depends on settings of collimators (“hierarchy”; machine protection rules).
- Yellow area corresponds to $> 90\%$ of proton tag chance.
- Scattered protons usually (distribution is process-dependent) have p_T around 0.2 GeV.
- Left: detectors located around 195 m: $0.17 \lesssim \xi \lesssim 0.31$.
- Center: detectors located around 217 m: $0.1 \lesssim \xi \lesssim 0.19$.
- Right: detectors located around 234 m: $0.06 \lesssim \xi \lesssim 0.09$.

- Acceptance in ξ translates into the acceptance in mass (note: process dependent as integral sensitive to p_T).
- Figure: mass acceptance of all pots and all pots combinations for the case of horizontal crossing angle ($\phi=0$):
 - “RP1” indicates that both the protons are tagged at the pot RP1A and RP1B (similarly for RP2 and RP3),
 - “RP1+RP2” means both protons are tagged at any two of the four pot locations RP1A, RP1B, RP2A and RP2B (similarly “RP1+RP3” and “RP2+RP3”),
 - “RP1+RP2+RP3” indicates that protons are tagged at any two stations on each side.



- I was asked to 'squeeze' physics case and focus on other topics in this presentation.
- For the real overview, please take a look at [Physics opportunities of ATLAS Forward Proton at the High-Luminosity LHC](#) [47 pages, on CDS]:
 - detailed ATLAS simulations:
 - WW (fully leptonic) + EFT study, WW (semi-leptonic), ZZ,
 - various ξ ranges; ToF of 10 and 20 ps,
 - based on ongoing Run 2 analyses: ALP searches ($0.035 < \xi < 0.08$; single-tag),
 - phenomenological studies:
 - semi-exclusive $t\bar{t}$: $0.015 < \xi < 0.15$, 10ps,
 - DM searches: $0.015 < \xi < 0.15$, 10ps,
 - exclusive Higgs in SM and BSM: $0.002 < \xi < 0.20$ (420 station considered), 10ps,
 - exclusive dijets: $0.02 < \xi < 0.12$, 10 ps.
- AFP is an asset to the ATLAS physics programme by providing additional handles for kinematic reconstruction and background rejection.
- From detailed simulations for single-tag AFP + ITk + HGTD configurations:
 - comparable significances observed to those based on central detector only,
 - higher S/B \rightarrow may indicate lower background modelling uncertainties.
- RP1 + RP3 is optimum if only eight stations can be installed.

An Initial Design Report for ATLAS Forward Proton Detectors at the High-Luminosity LHC was sent to a Review Panel called by the ATLAS Upgrade Coordinator on 22 Sep 2022:

- The main review meeting took place on 26/27 September.
- The Review Panel report with recommendations was issued on 10 October: **the main recommendation to ATLAS is not to approve the development of an AFP upgrade program for HL-LHC for Run 4, but to reserve the space for possible Run 5 or beyond projects if this is possible for the machine w/o constraints or additional cost.**
- The USC endorsed the Review Panel report and its recommendations at its meeting on 13 October 2022.
- The Executive Board approved the Review Panel report and its recommendations at its meeting on 17 October 2022.
- The result has been reported to and accepted by the HL-LHC Coordination Group (HLCG) on 18 October 2022.

- AFP was upgraded during LS2:
 - production of new tracking modules,
 - new design of detector flange: Out-of-Vacuum solution for ToF detectors,
 - new photo-multipliers: address inefficiency issues from Run2 data-taking,
- High and low- μ datasets collected in 2016 (one arm), 2017 and 2022:
 - performance studies close to be finalized,
 - analyses ongoing.
- No Roman Pots in ATLAS during Run 4.